Chemie der Erde 77 (2017) 587–595

Contents lists available at ScienceDirect

Chemie der Erde

journal homepage: www.elsevier.com/locate/chemer

Compositional variability of spinel-group minerals from the shergol serpentinized peridotites along indus suture zone, ladakh himalaya (India): constraints on tectonomagmatic history

Irfan Maqbool Bhat[a,*], Talat Ahmad[b], D.V. Subba Rao[c]

[a] Department of Earth Sciences, University of Kashmir, Srinagar, 190006, India
[b] Vice Chancellors Office, Jamia Millia Islamia, New Delhi, 110025, India
[c] Geochemistry Division, National Geophysical Research Institute (NGRI), Hyderabad, 500606, India

ARTICLE INFO

Keywords:
Ladakh himalaya
Shergol peridotites
Cr-spinel chemistry
Melt-rock interaction

ABSTRACT

The Shergol ophiolitic peridotites along ISZ, Ladakh Himalaya are serpentinized to various degrees and are harzburgite in composition. Electron microprobe analyses of spinels from Shergol Serpentinized Peridotites (SSPs) were carried out in order to evaluate their compositional variation with alteration. Chemical discontinuity was observed from core to rim in analyzed spinel grains with Cr-rich cores rimmed by Cr-poor compositions. From unaltered cores to rims it was observed that Cr^{3+}# and Fe^{3+}# increases while Mg^{2+}# decreases due to $Mg^{2+} - Fe^{2+}$ and Al^{3+} (Cr^{3+}) $- Fe^{3+}$ exchange with surrounding silicates during alteration. These peridotites contain Al-rich spinels forming subhedral to anhedral grains with lobate and corroded grain boundaries; altered to ferritchromite or magnetite along cracks and boundaries by later metamorphism episode. The unaltered Cr-spinel cores are identified as Al-rich and are characterized by lower values of Cr^{3+}# (0.34–0.40), high Al^{3+}# (0.58–0.68) and Mg^{2+}# (0.52–0.70). Mineral chemistry of these Al-rich Cr-spinels suggest that host peridotites have an affinity to abyssal and alpine-type peridotites. High TiO_2 concentration of magmatic Cr-spinel cores are in agreement with MORB melt-residual peridotite interaction. Presence of unaltered magmatic Cr-spinel cores suggest that they do not have re-equilibrated completely with metamorphic spinel rims and surrounding silicates. Cr-spinel core compositions of SSPs suggest an ophiolitic origin derivation by low degrees of melting of a less-moderate depleted peridotite in a mid-ocean ridge tectonic setting. Based on textural and chemical observations the alteration conditions of studied spinel-group minerals match those of transitional greenschist-amphibolite facies metamorphism consistent with estimated metamorphic equilibration temperature of ~ 500–600 °C.

1. Introduction

The mineral chemistry of chromite or chromian spinel (Cr-spinel) is important in reflecting parent magma chemistry, degrees of partial melting, melting behavior of the mantle and variation in fO_2 (Dick and Bullen, 1984; Arai, 1994; Zhou et al., 1996; Barnes, 2000; Hellebrand et al., 2002; Farahat, 2008; Aswad et al., 2011). It also plays an important role in classifying mantle derived peridotites in terms of geotectonic setting (Arai, 1992, 2011; Zhou et al., 1997; Arai et al., 2006) and is recognized as a sensitive mineral for deducing the physico-chemical parameters such as temperature, pressure, fO_2 etc. during magma crystallization (Roeder and Reynold, 1991; Zhou and Kerrich, 1992). Primary mineral compositions, particularly that of spinels of upper mantle peridotites, are a key to constrain the extent of partial melting, fluid phase enrichment, and mantle-melt interaction processes subsequent to melt extraction (Bonatti and Michael, 1989; Zhou et al., 1996, 2005; Hellebrand et al., 2001; Farahat, 2008; Choi et al., 2008; Aswad et al., 2011). In peridotites the primary Cr-spinel is resistant against alteration and metamorphism and partly preserved to give primary petrological characteristics (Matsumoto et al., 1997; Farahat, 2008).

The primary composition of spinel-group minerals, particularly of Cr-spinel, is susceptible to chemical modifications related to sub-solidus equilibration during metamorphism and hydrothermal processes (Kimball, 1990; Barnes, 2000; Farahat, 2008). Hydrothermal fluids ingress along cracks and around grain boundaries of primary Cr-spinel grains and produce Fe-enriched spinel (ferritchromite) and magnetite rims surrounding unaltered Cr-spinel core compositions (Barnes, 2000;

* Corresponding author at: Department of Earth Sciences, University of Kashmir, Srinagar, 190006, India.
E-mail address: imbhat89@gmail.com (I.M. Bhat).

http://dx.doi.org/10.1016/j.chemer.2017.10.003
Received 1 May 2017; Received in revised form 10 October 2017; Accepted 10 October 2017

Karipi et al., 2007; Farahat, 2008). Fluid-rock interaction causes exchange of cations between Cr-spinel and surrounding silicates and is temperature dependent. Exchange of divalent ions (Fe^{2+}, Mg^{2+}) readily occurs through greenschist to lower amphibolite facies whereas trivalent ions (Cr^{3+}, Al^{3+}, Fe^{3+}) remain unaltered up to lower amphibolite conditions (Farahat, 2008).

This paper presents new mineral chemistry data of spinel-group minerals from Shergol ophiolitic peridotites along Indus Suture Zone (ISZ), Ladakh Himalaya and aims to investigate the tectonomagmatic history of host peridotites.

2. Geological setting

The ISZ is the India-Asia convergence zone (Gansser, 1964, 1980; Frank et al., 1977; Thakur, 1981; Searle, 1983; Searle et al., 1987; Honegger et al., 1989; Cannat and Mascle, 1990) and is characterized by the ophiolitic relics of the Neo-Tethys, paleo-accretionary prism and mélange zone rocks of Cretaceous to Tertiary time (Brookfield and Reynolds, 1981; Raz and Honegger, 1989; Corfield et al., 1999; Robertson, 2000). In north-western Ladakh Himalaya, the ISZ is characterized by two groups of ophiolites and their associated paleo-accretionary prisms (Fig. 1a). The southern group is called the South Ladakh ophiolites viz. Nidar and Spontang ophiolites and their associated south Ladakh ophiolitic mélange; while the northern group is Dras ophiolite and its associated Sapi-Shergol mélange or southern mélange zone of Robertson (2000) (Maheo et al., 2006). These two mélange zones originated as two distinct Neo-Tethyan oceanic domains closed along two distinct north dipping subduction zones as evidenced by differences in their stratigraphy (Corfield et al., 1999; Robertson, 2000; Mahéo et al., 2004; Maheo et al., 2006); geochemical character and formation ages of two ophiolite groups (Reuber, 1986; Reuber et al., 1990; Ahmad et al., 1996, 2008; de Sigoyer et al., 2000; Corfield et al., 2001; Pedersen et al., 2001; Mahéo et al., 2004; Maheo et al., 2006).

In Ladakh region, the Sapi-Shergol mélange zone preserves the slices of ophiolites in the paleo-accretionary prism (Gansser, 1964; Frank et al., 1977; Honegger et al., 1982; Sinha and Mishra, 1992; Maheo et al., 2006). The Shergol paleo-accretionary prism consists of relics of sedimentary units and basic rocks of blueschist grade metamorphism (Frank et al., 1977; Virdi et al., 1977; Thakur, 1981; Searle, 1983; Honegger et al., 1989; Sinha and Mishra, 1992; Robertson, 2000; Maheo et al., 2006). The sedimentary unit is dominated by Upper Cretaceous turbidites intercalated with blocks of limestones, radiolarites, ultrabasic and basic rocks of greenschist grade metamorphism (Shah and Sharma, 1977; Honegger et al., 1989; Cannat and Mascle, 1990; Clift et al., 2000). The blueschists occur in a single and continuous SW-NE trending unit and show protolith geochemical signature of ocean island basalt (OIB) and enriched mid ocean ridge basalt (E-MORB) (Honegger et al., 1989; Sinha and Mishra, 1992, 1994; Robertson, 2000), whereas OIB represent relics of Late Cretaceous seamounts within the Neo-Tethys ocean which were eroded and incorporated into the accretionary prism during Late Cretaceous intra-oceanic subduction (Honegger et al., 1982, 1989; Sinha and Mishra, 1992). This blueschist unit is overlain by Shergol continental conglomerate of Oligo-Miocene age (Honegger et al., 1989; Cannat and Mascle, 1990; Robertson, 2000; Maheo et al., 2006).

The Shergol serpentinized peridotites (SSPs) are situated along ISZ, NW Ladakh Himalaya. At Shergol village (30 km south-east of Kargil district along Srinagar-Leh National highway), the blocks of massive and unsheared serpentinized peridotites float in a matrix of highly sheared serpentinite forming the classic block-in-matrix texture (Fig. 1b). Despite partial to extensive serpentinization, these peridotite blocks differ from the sheared serpentine matrix in preserving their primary mantle textures and mineral compositions. Based on the relic mineralogy, these massive blocks represent protolith of harzburgite composition. The geochemical study suggest that SSPs represent melting residues remaining after low to moderate degrees of partial melting (< 15%) of moderately fertile lherzolite at mid ocean ridge tectonic setting in the context of ancient Mesozoic Neo-Tethyan oceanic mantle which was subsequently trapped in the accretionary complex of Ladakh magmatic arc (Bhat et al., 2017). To unravel the magmatic history of these peridotite tectonic blocks (knockers), we use major element composition of relic spinel group mineral phases. For partially or highly serpentinized peridotites, mineral composition of spinel is especially useful as it is typically unaffected by the serpentinization process, except forming magnetite or ferritchromite rims along grain boundaries and fractures.

3. Petrography of shergol serpentinized peridotites

The SSPs are porphyroclastic in texture and display solid-state deformation structures of undulose extinction, kink bands, shearing and recrystallization characteristic features of alpine type or ophiolite upper mantle peridotites. The SSPs are serpentinized to various degrees, which resulted in the pseudomorphic textures of mesh and hourglass after olivine and bastites after pyroxene (Bhat et al., 2017). They contain < 2 mm long red brown colored holly leaf-shaped or type 1 spinels (Fig. 2a) that are associated with orthopyroxene and also isolated subhedral or type 2 spinels (Fig. 2b and c) and euhedral or type 3 spinels (Fig. 2d). At places, spinels show corroded texture with highly irregular shape. In order to distinguish various zones of spinels, back-scattered electron (BSE) images were employed by using the contrast function. Due to hydrothermal alteration, the spinel-group of minerals gradually transform to ferritchromite and then to magnetite which is considered to be the final end product (Paraskevopoulos and Economou, 1980). The effect of alteration/metamorphism on studied spinel grains is evident in BSE images with various concentric shades; darker at the core and brighter at the rim of spinel grains. The Cr-spinel core composition preserves the primary characteristics and is mantled by ferritchromite and magnetite zones of irregular shapes (Fig. 2c and d). Some primary spinel grains are completely replaced by ferritchromite and mantled by magnetite rims (Fig. 2e) whereas commonly encountered primary spinel grains are mantled with rim of magnetite, this could be the result of variation in grade of metamorphism (Kapsiotis et al., 2007). At higher metamorphic temperatures, primary Cr-spinel alters to ferritchromite while at lower temperature it alters to magnetite (Lee, 1999; Ahmed et al., 2001). The secondary silicate assemblage in SSPs mainly includes serpentine (60–70%) and variable percentage of chlorite and magnetite. Accessory pentlandite (an Fe-Ni sulfide) occurs too (Fig. 2f) which typically develops during serpentinization as Fe content decreases and Ni increases in sulphides during such process (Shiga, 1987).

4. Analytical methods

Twenty thin sections of harzburgite samples from Shergol ophiolitic slice, Ladakh Himalaya were examined using a polarizing, transmitted light microscope equipped with a digital camera. Out of these, twelve samples were analyzed for spinel mineral chemistry using Electron Probe Micro Analyzer (EPMA) CAMECA SX-Five instrument at the Banaras Hindu University, Varanasi, India. Selected spinel grains in thin sections were analyzed along profile lines in order to determine the compositional variation. For spinel group minerals, CAMECA SX-Five instrument was operated by SX-Five Software at an accelerating voltage of 15 kV and a probe current of 10–20 nA. Quality control was maintained by analyzing well calibrated natural materials/minerals as standards (chromite for Cr, hematite for Fe and NiO for Ni) during each electron microprobe session. The proportion of ferrous and ferric iron in spinels was calculated by assuming spinel stoichiometry. Routine X-ray spectral analysis (calibration, acquisition, quantification) and data processing was carried out using SxSAB version 6.1 and SX-Results software's of CAMECA and replicate analyses of individual points show

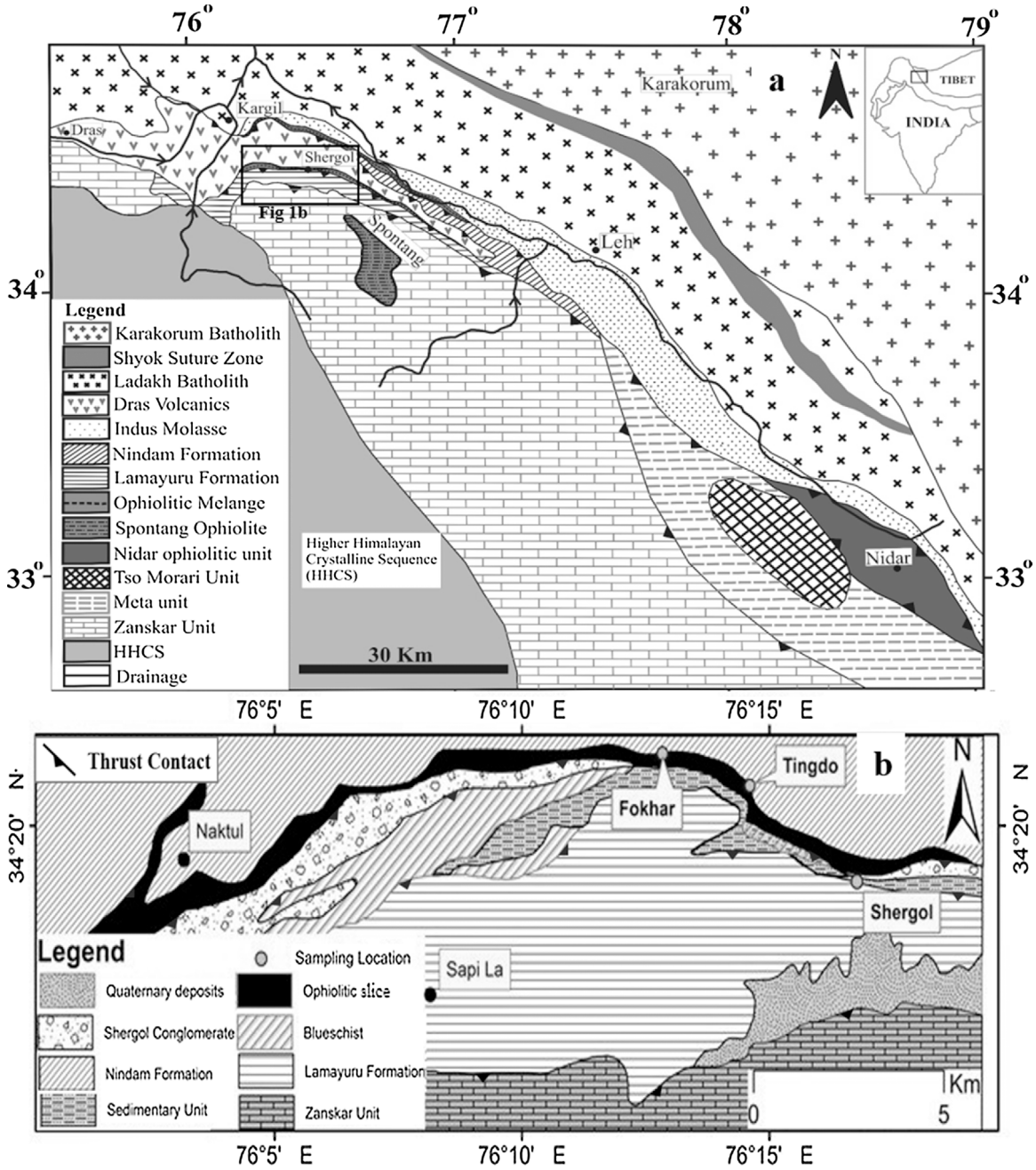

Fig. 1. (a) Geological map of the Ladakh Himalaya (after Mahéo et al., 2004), showing location of the study area, (b) Geological map of the Sapi-Shergol ophiolitic slice along Indus suture zone, Ladakh Himalaya showing sampling locations (after Honegger et al., 1989).

analytical error of < 2%.

5. Compositional variability in spinel group minerals from SSPs

Representative mineral chemistry of the spinel group minerals from SSPs is given in Tables 1 and 2, but in the following plots, we have also used Cr-spinel data from Bhat et al. (2017). Variability in spinel group mineral compositions from SSPs is illustrated in $Al^{3+} - Cr^{3+} - Fe^{3+}$ triangular diagram (Fig. 3). Cr-spinel, ferritchromite and magnetite are the common spinel group minerals found in SSPs.

In $Al^{3+} - Cr^{3+} - Fe^{3+}$ triangular plot three compositional variability zones distinctively characterize spinel group minerals of SSPs. The ferritchromite and magnetite rims mantling the primary Cr-spinel cores are of metamorphic origin. From the microprobe analysis, it was observed that the ferritchromite and magnetite are highly depleted in Al^{3+} and Mg^{2+} as compared to Cr-spinel core. Cr^{3+} shows slight depletion in ferritchromite relative to core but is highly depleted in magnetite. Fe^{2+} and Fe^{3+} are the only elements which are significantly enriched at the rim compared to the unaltered core. Mn and Si show relative enrichment in ferritchromite compared to Cr-spinel core and magnetite rim. Based on these compositional variabilities it is suggested that Fe and to a lesser extent Mn and Si are introduced into the Cr-spinel however, Al, Mg and Cr diffuse out of the Cr-spinel during alteration and metamorphism. This chemical variability further confirms the presence of two compositional miscibility gaps, one between Cr-spinel core and ferritchromite and other between ferritchromite zone and magnetite rim as was observed in Fig. 3. In peridotites, due to extensive $Mg^{2+} - Fe^{2+}$ exchange between coexisting spinel and silicate phases, Mg# [cationic ratio of $Mg^{2+}/(Mg^{2+} + Fe^{2+})$] rapidly decreases from Cr-spinel core through ferritchromite to magnetite rim

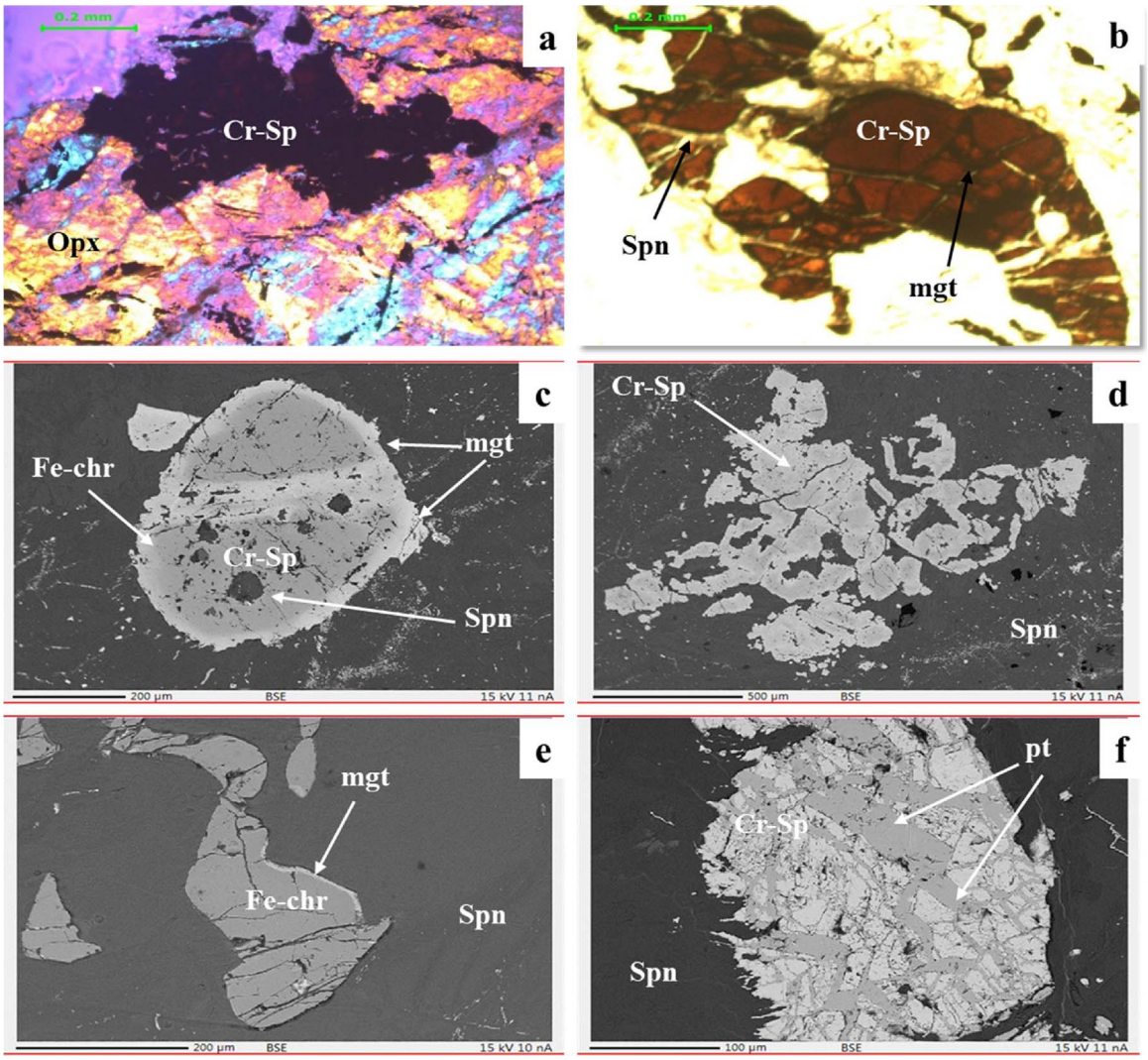

Fig. 2. Photomicrographs and back scatter electron (BSE) images of spinel grains from SSPs (a) irregular spinel grains under crossed polarized light, (b) highly corroded and fractured spinel grain showing development of magnetite (mgt) along fractures, (c) SEM photograph of a zoned spinel grain with Cr-spinel (Cr-Sp) core followed by ferrochromite (Fe-chr) and a thin film of magnetite (mgt) at the rim, (d) SEM photograph of a highly fractured spinel surrounded by a serpentine groundmass, (e) SEM photograph of a subhedral ferrochromite (Fe-Chr) grain showing thin film of magnetite (mgt) and (f) SEM photograph of a subhedral grain of pentlandite (pt) in a serpentine (spn) groundmass.

(Fig. 4a). However, Fe^{3+}# [(cationic ratio of $Fe^{3+}/(Fe^{3+} + Cr^{3+} + Al^{3+})$] increases with decreasing Mg# from Cr-spinel core to the magnetite rim (Fig. 4b) because of Al^{3+} loss and Fe^{3+} enrichment during alteration and metamorphism.

The cores of altered spinels in SSPs are primary in origin with Cr-spinel composition and are characterized by low Cr_2O_3 (28.47–32.66 wt.%), high Al_2O_3 (32.49–39.18 wt%) and MgO (10.43–15.88 wt%). TiO_2 content varies from 0.02 to 0.30 wt.% and is comparable to that of alpine and abyssal peridotites (Arai, 1992; Farahat, 2008; Aswad et al., 2011). This Cr-spinel data when plotted in a ternary triangular plot of $Al^{3+} - (Fe^{3+} + 2Ti^{4+}) - Cr^{3+}$ shows affinity towards alpine peridotites (Fig. 5). The magma composition of ultramafic rocks from which spinel-group minerals crystallize defines their chemistry, hence the mineral has the potential to reflect the chemical character of the parent magma (Irvine, 1967; Dick and Bullen, 1984; Allen et al., 1988; Roeder and Reynold, 1991; Arai, 1992; Zhou et al., 1994). The analyzed Cr-spinels have Cr^{3+}# [cationic ratio of $Cr^{3+}/(Cr^{3+} + Al^{3+})$] = 0.34–0.40, which is comparable to mid-ocean ridge tholeiitic parent magma of 0.20–0. 54 (Allen et al., 1988) and are lower than those of layered igneous intrusions of Bushveld and Stillwater which have Cr# = 0.70–0.85 (Irvine, 1967) and those of boninite magmas of 0.80–0.90 (Roeder and Reynold, 1991). The Cr-spinel data of SSPs plotted in Al_2O_3 vs. TiO_2 binary plot in comparison to modern day tectonic settings shows affinity towards abyssal peridotites as compared to supra-subduction zone peridotites (Fig. 6).

6. Discussion

6.1. Metamorphic alteration effects on spinel-group mineral compositions

The extent of alteration of the primary spinels is a function of metamorphic grade and fluid-rock ratio, hence the post magmatic alteration processes (hydrothermal alteration) of the host peridotites may result in some of the chemical variability in spinel-group mineral compositions (Barnes, 2000; Farahat, 2008; Aswad et al., 2011). Depending on the extent of alteration, ferritchromite and/or Cr-magnetite as secondary phases will start to form and are usually attributed to the effects of low- to medium-grade metamorphism up to lower amphibolite facies (Thalhammer et al., 1990; Kapsiotis et al., 2007; Farahat 2008). The microprobe analyses of Cr-spinels from SSPs reflect Cr-rich core and development of ferritchromite and magnetite rims as common alteration products. Magnetite forms films and fracture fillings in spinels (Fig. 2c), which is the consequence of exchange of Mg^{2+} and Fe^{2+} cations between spinel-group minerals and coexisting silicates,

Table 1
Representative electron-microprobe analyses of Cr-spinel core compositions (recalculated on 32 Oxygen basis) from Shergol serpentinized peridotites along ISZ, NW Ladakh Himalaya.

	Cr-Spinel							
wt.%	P-92	P-143	P-77	P-78	P-270	P-271	P-274	P-275
SiO_2	0.08	0.04	0.66	0.47	0.12	0.12	0.97	0.11
TiO_2	0.02	0.04	0.30	0.15	0.14	0.15	0.18	0.16
Al_2O_3	35.22	36.73	39.18	32.49	35.60	34.42	34.50	35.34
Cr_2O_3	30.91	28.47	30.26	32.52	31.43	32.66	29.47	31.29
Fe_2O_3	4.56	5.02	0.10	3.34	2.84	3.43	3.80	3.64
FeO	13.41	14.67	17.45	17.05	13.50	13.20	14.60	13.48
MnO	1.73	1.54	1.72	1.82	0.24	0.27	0.76	0.33
MgO	14.68	14.14	10.33	12.49	15.71	15.88	15.28	15.75
Total	100.46	100.50	99.89	100.33	99.59	100.12	99.55	100.10
Si^{4+}	0.02	0.01	0.15	0.11	0.03	0.03	0.22	0.03
Ti^{4+}	0.00	0.01	0.05	0.03	0.03	0.03	0.03	0.03
Al^{3+}	9.59	9.97	10.80	9.05	9.68	9.35	9.43	9.58
Cr^{3+}	5.65	5.19	5.60	6.08	5.73	5.95	5.40	5.69
Fe^{3+}	0.79	0.87	0.00	0.59	0.49	0.59	0.66	0.63
Fe^{2+}	2.59	2.83	3.41	3.37	2.60	2.54	2.83	2.59
Mn^{2+}	0.34	0.30	0.34	0.37	0.05	0.05	0.15	0.06
Mg^{2+}	5.05	4.86	3.64	4.40	5.40	5.46	5.28	5.40
Cr^{3+}#	0.37	0.34	0.34	0.40	0.37	0.39	0.36	0.37
Mg^{2+}#	0.66	0.63	0.52	0.57	0.61	0.59	0.61	0.60
Al^{3+}#	0.60	0.62	0.66	0.58	0.67	0.68	0.65	0.68
Fe^{3+}#	0.05	0.05	0.00	0.04	0.03	0.04	0.04	0.04
Fe^{2+}#	0.34	0.37	0.48	0.43	0.33	0.32	0.35	0.32

$Cr^{3+}\# = Cr^{3+}/[Cr^{3+} + Al^{3+}]$; $Al^{3+}\# = Al^{3+}/(Cr^{3+} + Al^{3+} + Fe^{3+})$; $Fe^{3+}\# = Fe^{3+}/(Cr^{3+} + Al^{3+} + Fe^{3+})$; $Mg^{2+}\# = Mg^{2+}/[Mg^{2+} + Fe^{2+}]$; $Fe^{2+}\# = Fe^{2+}/(Fe^{2+} + Mg^{2+})$.

particularly olivine (Barnes, 2000; Karipi et al., 2007; Farahat, 2008). The common preservation of magmatic Cr-spinel cores in SSPs implies low fluid-rock ratio/interaction during hydrothermal alteration. With continuous fluid-rock interaction, some Cr-spinel cores equilibrate with surrounding silicate minerals and alter to ferritchromite, despite the presence of magnetite rims. These ferritchromite cores surrounded by magnetite rims (Fig. 2e) were grown by diffusive replacement of Mg^{2+} by Fe^{2+} in the spinel structure. Via this process, the altered spinels (ferritchromite and magnetite) in SSPs display lower Mg# but higher Cr# and Fe^{3+}# than unaltered Cr-spinel cores (Fig. 4). This chemical

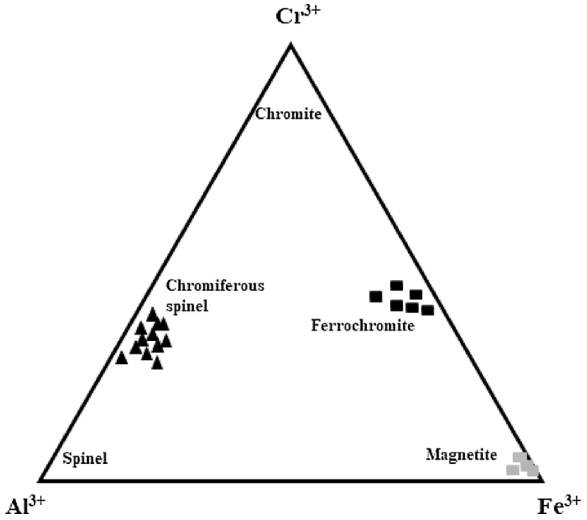

Fig. 3. Trivalent cation classification triangular diagram showing the compositional variation of spinel-group minerals from SSPs.

variation is due to preferential retention of Cr in unaltered Cr-spinels while its breakdown/alteration provides Al for secondary chlorite (Kimball, 1990; Karipi et al., 2007). Barnes (2000) suggested that the metamorphic grade of hydrothermal alteration effectively controls the $Mg^{2+}/(Mg^{2+} + Fe^{2+})$ ratios in altered compositions of spinel-group minerals. Rocks altered under greenschist facies of metamorphism have spinels with Mg# ranging from 0.4 to 0.7, while amphibolite facies rocks have Mg# < 0.35 (Barnes, 2000; Farahat, 2008). The $Mg^{2+}/(Mg^{2+} + Fe^{2+})$ ratio in the studied spinels ranges from 0.5 − 0.7, reflecting green schist grade of metamorphism.

The compositional variability of spinel-group minerals from SSPs in relation to metamorphic temperature conditions is shown in Fig. 7. The Cr-spinel core compositions plot outside the 600 °C stability limit of Sack and Ghiorso (1991), reflecting primary relic magmatic nature not affected by alteration/metamorphism. However, metamorphic spinels, i.e., ferritchromite and magnetite equilibrated around ~ 500 − 600 °C lie along the Cr^{3+} − Fe^{3+} join with additional compositional/miscibility gap. The primary Cr-content is retained in Cr-spinels

Table 2
Representative electron-microprobe analyses of Ferritchromite and magnetite (rim composition) from Shergol serpentinized peridotites along ISZ, NW Ladakh Himalaya.

	Ferritchromite						Magnetite					
wt.%	P-57	*P*-38	*P*-34	P-75	P-82	P-71	P-24	P-7	P-11	P-148	P-152	P-144
SiO_2	6.82	7.37	7.88	6.24	2.85	3.52	0.06	0.15	0.02	0.39	0.80	0.14
TiO_2	0.23	0.36	0.12	0.28	0.55	0.38	0.14	0.12	0.05	0.00	0.06	0.07
Al_2O_3	2.13	1.70	4.15	2.74	0.76	1.14	0.20	0.34	0.10	0.00	0.10	0.12
Cr_2O_3	22.52	25.44	26.16	25.10	27.87	24.88	0.16	0.15	0.10	0.12	0.09	0.11
Fe_2O_3	31.51	27.34	23.71	28.98	34.01	36.92	66.50	67.82	67.90	68.37	67.30	67.98
FeO	21.65	23.18	21.52	22.84	21.88	20.81	30.30	31.00	30.12	30.27	30.08	30.72
MnO	7.28	7.07	7.57	6.75	8.57	5.90	0.15	0.19	0.26	0.39	0.16	0.18
MgO	7.86	7.55	8.89	7.07	3.51	6.45	0.10	0.12	0.23	0.30	0.91	0.16
Total	100.00	100.00	100.00	100.00	100.00	100.00	97.35	99.89	98.76	99.84	99.50	99.47
Si^{4+}	1.88	2.03	2.13	1.73	0.83	1.00	0.02	0.01	0.01	0.02	0.03	0.04
Ti^{4+}	0.05	0.07	0.02	0.06	0.12	0.08	0.04	0.04	0.01	0.01	0.02	0.02
Al^{3+}	0.69	0.55	1.32	0.89	0.26	0.38	0.01	0.02	0.01	0.02	0.01	0.04
Cr^{3+}	4.91	5.55	5.57	5.49	6.40	5.58	0.01	0.01	0.03	0.04	0.03	0.03
Fe^{3+}	6.54	5.68	4.81	6.04	7.44	7.88	1.97	1.96	1.99	1.97	1.93	15.81
Fe^{2+}	4.99	5.35	4.85	5.29	5.32	4.93	1.00	1.00	0.98	0.99	0.98	7.94
Mn^{2+}	1.70	1.65	1.73	1.58	2.11	1.42	0.01	0.01	0.01	0.01	0.05	0.05
Mg^{2+}	3.23	3.11	3.57	2.92	1.52	2.73	0.01	0.01	0.01	0.02	0.05	0.07
Cr^{3+}#	0.88	0.91	0.81	0.86	0.96	0.94	0.35	0.24	0.39	0.16	0.37	0.37
Mg^{2+}#	0.39	0.37	0.42	0.36	0.30	0.36	0.01	0.01	0.01	0.02	0.05	0.01
Al^{3+}#	0.06	0.05	0.11	0.07	0.02	0.03	0.00	0.01	0.00	0.01	0.00	0.00
Fe^{3+}#	0.54	0.48	0.41	0.49	0.53	0.57	0.99	0.99	1.00	0.99	1.00	1.00
Fe^{2+}#	0.61	0.63	0.58	0.64	0.78	0.64	0.99	0.99	0.99	0.98	0.95	0.99

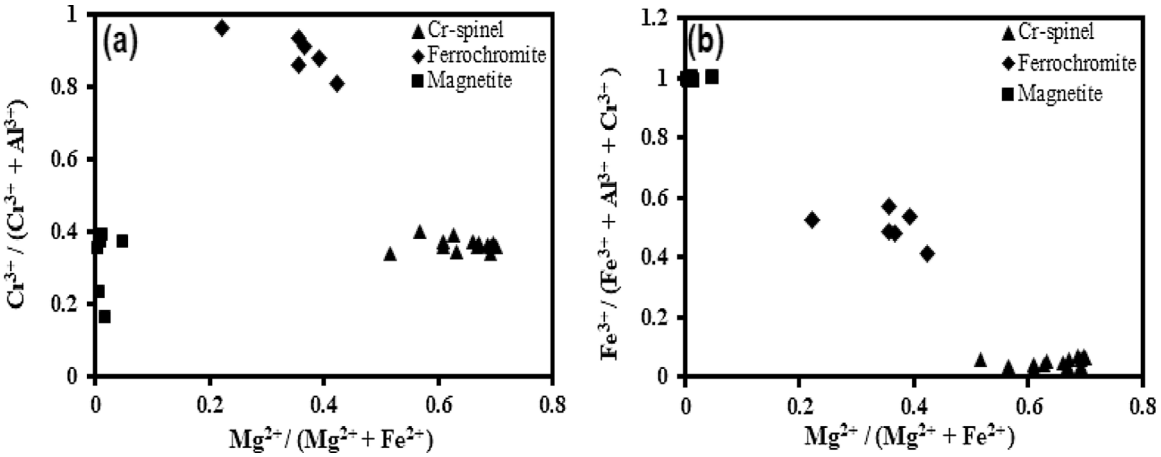

Fig. 4. Spinel-group mineral compositions from SSPs plotted in (a) $Cr^{3+}/(Cr^{3+} + Fe^{3+})$ against $Mg^{2+}/(Mg^{2+} + Fe^{2+})$ and (b) $Fe^{3+}/(Fe^{3+} + Al^{3+} + Cr^{3+})$ against $Mg^{2+}/(Mg^{2+} + Fe^{2+})$.

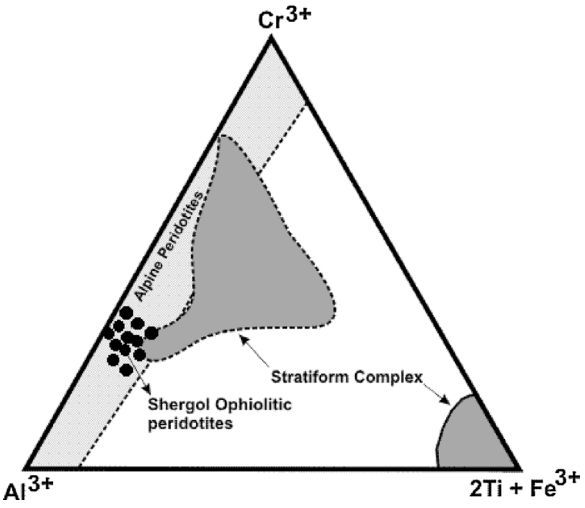

Fig. 5. Triangular trivalent cation plot of $Al^{3+} - (Fe^{3+} + 2Ti^{4+}) - Cr^{3+}$ (after Jan and Windley, 1990) for Cr-spinels from SSPs.

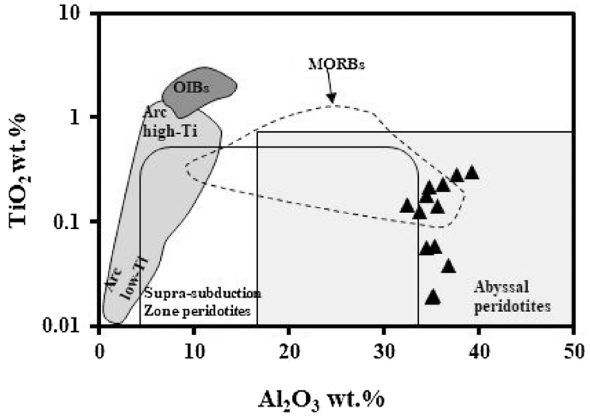

Fig. 6. Al_2O_3 vs. TiO_2 binary plot (after Kamenetsky et al., 2001) of Cr-spinels in comparison to modern-day tectonic settings.

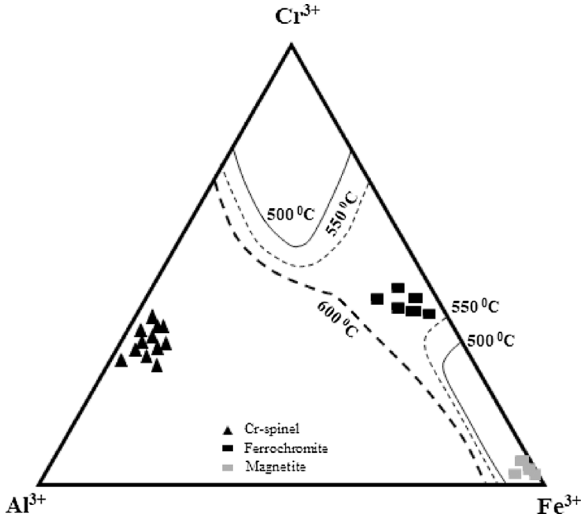

Fig. 7. Compositional variability in spinel-group minerals from SSPs in a triangular $Cr^{3+} - Fe^{3+} - Al^{3+}$ plot. Spinel stability limits for Cr-spinel, ferrochromite and magnetite (calculated for equilibrium with olivine of composition Fo_{90}) are after Stack and Ghiorso (1991).

equilibrated below ~ 500 − 550 °C stability limit but their Mg# is substantially lowered by $Fe^{2+} - Mg^{2+}$ exchange with surrounding silicates (Farahat, 2008). The magnetite rims are almost pure with limited Cr solubility, implying magnetite growth well below 500 °C. The present ferritchromite preserves high Cr_2O_3 (23 − 28 wt.%) close to those of unaltered Cr-spinel cores but has lower Mg#. Metamorphism of 550–600 °C grade substantially modifies the primary spinel composition through infiltrating metamorphic fluids (Wylie et al., 1987; Barnes, 2000). The high Mn-content of ferritchromite is owing to the ability of the Cr-spinel to act as a favorable Mn-receptor during serpentinization process as the secondary silicates (serpentine, chlorite) accommodate less Mn than their igneous precursors (Deer et al., 1992).

Due to greenschist grade of metamorphism in peridotites, magnetite alteration zones develop around margins with a sharp boundary and along fractures of Cr-spinel grains. These metamorphic/secondary rims become much wider with curved and lobate boundary and are concentrically zoned from Cr-poor (magnetite) to Cr-rich margins, Al-poor compositions (ferritchromite) at inner contact with Cr-spinel core at around transitional greenschist-amphibolite to lower amphibolite facies (Kapsiotis et al., 2007). Cr-spinel grains are almost completely replaced by magnetite and rare ferritchromite cores at mid-amphibolite grade of metamorphism (Farahat, 2008). In SSP spinels, the presence of magnetite or ferritchromite rims mantling Cr-spinel cores and complete replacement of Cr-spinel cores with ferritchromite mantled with magnetite provides textural evidence for greenschist to lower amphibolite facies alteration conditions and absence of complete replacement of Cr-spinel by magnetite precludes any higher metamorphic alteration grades such as mid-amphibolite or granulite facies metamorphism.

Thus, based on textural and chemical observations the alteration conditions of studied spinel-group minerals from SSPs match those of transitional greenschist-amphibolite facies metamorphism consistent with above estimated metamorphic equilibration temperature of ~ 500–600 °C.

6.2. Nature of shergol serpentinized peridotites

For the mantle derived spinel peridotites, Cr# of spinel is a proxy indicator for the degree of partial melting in the host rock. Cr-spinels with Al# > Cr# represent less depleted peridotites, whereas Cr# > Al# or high Cr# spinels reflect highly depleted peridotites (Dick and Bullen, 1984; Arai, 1994). Generally, primitive mantle peridotites contain spinels with Cr# of 0.8–0.10 (Cabanes and Mercier, 1988), which increases with the evolution of partial melting (Irvine, 1967; Bonatti and Michael, 1989; Hellebrand et al., 2001). The higher value of Cr# (0.34 − 0.40) of Cr-spinel in the studied peridotites relative to primitive mantle peridotites are thus consistent with imprint of a partial melting episode. These Cr-spinels have lobate grain boundaries and their affinity to abyssal peridotite spinels in terms of Cr#, Mg#, Al# and TiO_2 (Table 1) also suggest the involvement of a partial melting episode in their genesis. Also, Bhat et al. (2017) have shown that the SSPs reflect residual character after moderate degrees of melt extraction (< 15%) from a moderately fertile mantle source at mid-ocean ridge tectonic setting based on depletions in their whole rock incompatible and heavy rare earth elements and existence of high-Al low-Cr spinels comparable to abyssal peridotites.

6.3. Post melting melt-rock reaction

Post-melting melt-rock interaction due to percolating and/or impregnating melts typically changes the chemical composition of the residual mantle peridotites and associated chromites (Zhou et al., 1996; Parkinson and Pearce, 1998; Pearce et al., 2000; Dare et al., 2009), thereby increasing concentration of Ti in existing chromites (Edwards and Malpas, 1995) and clinopyroxenes (Zhou et al., 2005) and/or crystalizing high-Al and high-Cr podiform chromitites (Zhou et al., 1994, 1996; Melcher et al., 1997). Abyssal peridotites are not simple melting residues but mostly are reacted or refertilized to some extent which results either from melt-rock reaction or impregnated melts which are not able to leave the mantle source (Niu et al., 1997; Niu, 1997, 2004). Cr-spinels associated with these peridotites (including back-arc peridotites) have generally low Cr# (< 0.6: Dick and Bullen, 1984; Arai and Miura, 2015). Interaction of mantle peridotites with mid-ocean ridge basalt (MORB) melts results in enrichment of TiO_2 but no increase of Cr# in Cr-spinels (Pearce et al., 2000; Choi et al., 2008; Shervais et al., 2011). Cr-spinels related to subduction zone magmas are characterized by high Cr# (> 0.6) and low Ti because of higher degrees of partial melting (Dick and Bullen, 1984; Arai, 1992; Arai and Yurimoto, 1995; Arai et al., 2006). The occurrence of high-Cr and high-Ti Cr-spinel is characteristic of highly refractory peridotites formed in a supra-subduction setting by hydrous melt extraction (Pearce et al., 2000; Choi et al., 2008; Shervais et al., 2011) and by melt-rock reaction (Zhou et al., 1996, 2005, 2014; Xiong et al., 2015, 2017a). Melt-rock reaction in supra-subduction zones was observed in Yarlung-Zangbo Suture Zone ophiolites of Tibet such as Luobusa peridotites (Zhou et al., 1996; Xiong et al., 2014, 2015), Xigaze peridotites (Xiong et al., 2017a) and Dongbo peridotites (Xiong et al., 2017b) and podiform chromitites of Guleman ophiolite, SE Turkey (Rizeli et al., 2016).

The occurrence of subhedral to euhedral Cr-spinel grains with relatively high Ti concentration of some Cr-spinel grains in SSPs can be explained by a melt-rock interaction episode (Arai, 1992; Zhou et al., 1996; Pearce et al., 2000). The plot of Cr# versus TiO_2 (for spinels) is particularly effective in distinguishing between partial melting and post melting melt-rock interaction processes experienced by the host peridotite (Pearce et al., 2000). The Cr-spinel data from SSPs, when plotted

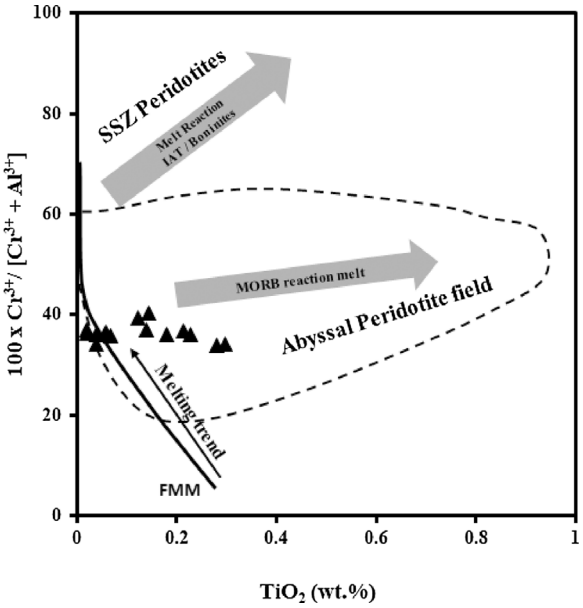

Fig. 8. Plot of TiO_2 against Cr# (after Pearce et al., 2000) of Cr-spinels from SSPs. The diagram discriminates between residual and reacted peridotites. Melting trend modeled by Pearce et al. (2000) from fertile MORB mantle (FMM), dotted line field for abyssal peridotite spinels, MORB reaction melt arrow reflect MORB-melt reacted abyssal peridotite spinels and IAT/Boninite reaction melt arrow reflect supra-subduction zone (SSZ) refractory peridotite spinels. (MORB: mid-ocean ridge basalt; IAT: island arc tholeiite).

in Cr# vs. TiO_2 diagram of Pearce et al. (2000), some points follow the melting trend but others deviate right to the melting trend (Fig. 8). Because of low diffusivity of Ti in olivine as compared to spinel, Ti concentration in Cr-spinel is not only sensitive to melt-rock reaction process but can fingerprint the composition of the interacting melts (Scowen et al., 1991; Pearce et al., 2000). In abyssal peridotites, melt extraction results in TiO_2 depletion (< 0.1 wt.%) but increase in Cr# (≤0.6) in associated Cr-spinels. When these residual peridotites later react with MORB composition melts (Ti-rich), their spinels become enriched in TiO_2 without increasing their Cr# (Kelemen et al., 1995; Pearce et al., 2000) whereas, reaction with boninite melts results in high-Cr and high-Ti spinels (Zhou et al., 1996, 2005, 2014; Pearce et al., 2000; Choi et al., 2008; Shervais et al., 2011; Xiong et al., 2015, 2017a). This is the basis for fingerprinting the melt composition that interacted with the residual mantle in a specific tectonic setting. In Fig. 8, the investigated Cr-spinels plot in the MORB melt reaction field indicating that the interacting melt was of MORB composition. Some spinels in SSPs have low Ti contents typically < 0.06 wt.% but others have higher concentration of 0.1 − 0.3 wt.%. The lower and uniform Cr# (~ 0.34–0.40) but different Ti content of the studied spinels reflect complex origin of the host peridotites. The lower Ti-spinels plot within ± 0.05 wt.% TiO_2 of melting trend in Fig. 8, however, the high Ti-spinels are significantly displaced to the right of the melting trend suggesting that the host peridotites are not simple melting residues but the products of melt-rock reaction with Ti-rich melts (Pearce et al., 2000; Choi et al., 2008; Shervais et al., 2011; Cimen et al., 2016). The above interpretation is supported by the petrological/petrographic evidence of type 2 or subhedral and type 3 or euhedral spinels in these peridotites. It is thus summarized that the Cr-spinel morphology and chemistry from SSPs reveals a multi-stage genesis with an earlier partial melting event preserved in unreacted spinels followed by a subsequent episode of melt-rock interaction during their mantle stay at mid ocean ridge tectonic affinity and thus the SSPs are monogenetic peridotites.

6.4. Tectonic implications

In a spinel trivalent ternary cation plot (Fig. 9), the studied spinels

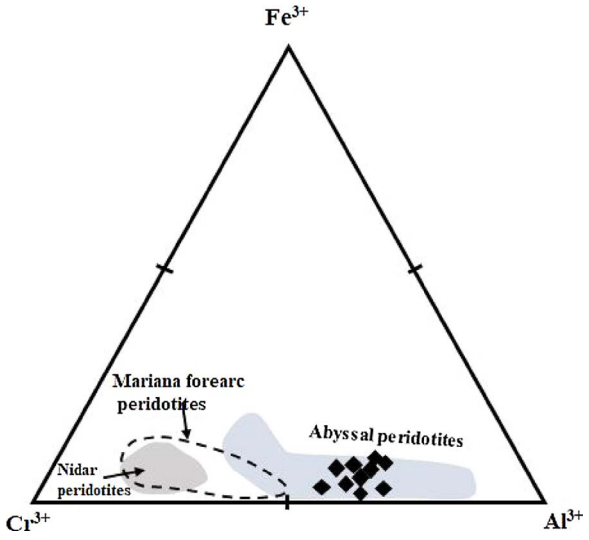

Fig. 9. Cr-spinel composition from SSPs (solid diamonds) plotted on triangular trivalent cation plot (Al^{3+} – Fe^{3+} – Cr^{3+}), in comparison to abyssal peridotites (field after Dick and Bullen, 1984; Barnes and Roeder, 2001), Mariana fore arc peridotites (dashed area after Ishii et al., 1992; Parkinson and Pearce, 1998) and Nidar peridotites or Himalayan serpentinites (dashed area after Hattori and Guillot, 2007).

plot in a field of abyssal peridotites in comparison to Cr-spinels from south Ladakh Himalayan serpentinites which show geochemical signatures similar to that of Mariana fore arc peridotites and reflect greater degrees of partial melting with of Cr# > 0.70 (Hattori and Guillot, 2007). On the basis of whole rock and spinel mineral chemistry, Bhat et al. (2017) have shown that the SSPs originated from a less to moderately depleted peridotite which underwent relatively moderate fractions of melt extraction (< 15% melting) based on the correlation between Cr# and the degree of melting from the modeled equation of Hellebrand et al. (2001), thus are consistent with worldwide abyssal peridotites (Bodinier and Godard, 2003; Niu, 2004; Singh, 2009; Delavari et al., 2009; Ningthoujam et al., 2012). Due to this variability in magmatic Cr-spinel chemistry, the SSPs reflect different geodynamic history than south Ladakh ophiolitic peridotites despite their occurrence along the Indus Suture Zone.

7. Conclusion

The spinel group minerals in SSPs are typically zoned with unaltered cores to Cr-magnetite rims through ferritchromite transitional zones. Compared to the cores, the rims are depleted in Al^{3+}, Mg^{2+}, and Cr^{3+} while enriched in Fe^{3+}. The Cr-spinel core compositions of SSPs have generally low TiO_2 (< 0.06 wt.%) content, but some spinels with intermediate Cr# are enriched in TiO_2 (up to 0.3 wt.%), indicating reaction with MORB-like melts. Based on the Cr-spinel morphology and chemistry, it is summarized that the SSPs reveal multi-stage genesis in their tectonomagmatic history with an earlier pre-serpentinization episode of partial melting event preserved in unreacted spinels followed by subsequent episode of post melting melt-rock interaction during their mantle stay at mid-ocean ridge tectonic environment. Consequently, syn- or post-serpentinization alteration/metamorphism episode of transitional greenschist-amphibolite grade effect SSPs thereby causing alteration of primary Cr-spinels to ferritchromite and magnetite as well as development of chlorite and serpentine from primary silicate minerals. Some of the Cr-spinel cores continued to equilibrate/communicate with the surrounding silicate minerals by exchanging Mg^{2+} and Fe^{2+} and were totally modified to ferritchromite with a rim of magnetite.

Acknowledgements

This work was supported by the Council of Scientific and Industrial Research (CSIR, New-Delhi) under senior research fellowship (SRF) grant to the first author. The authors are thankful to Prof. Shakil Ahmad Romshoo, Head, Department of Earth Sciences, University of Kashmir for giving permission to publish this work. Prof. N. V. Chalapathi Rao, Banaras Hindu University, Varanasi, India is thankfully acknowledged for EPMA analysis.

References

Ahmad, T., Islam, R., Khanna, P.P., Thakur, V.C., 1996. Geochemistry, petrogenesis and tectonic significance of the basic volcanic units of the Zildat ophiolitic melange, Indus suture zone, eastern Ladakh (India). Geodinamica Acta 9, 222–233.
Ahmad, T., Tanaka, T., Sachan, H.K., Asahara, Y., Islam, R., Khanna, P.P., 2008. Geochemical and isotopic constraints on the age and origin of the Nidar Ophiolitic Complex, Ladakh, India: implications for the Neo-Tethyan subduction along the Indus suture zone. Tectonophysics 451, 206–224.
Ahmed, A.H., Arai, S., Attia, A.K., 2001. Petrological characteristics of podiform chromitites and associated peridotites of Pan African Proterozoic ophiolite complex of Egypt. Miner. Deposita 36, 72–84.
Allen, J.F., Sack, R.O., Batiza, R., 1988. Cr-spinels as petrogenetic indicators MORB-type lavas from the Lamount seamount chain, eastern Pacific. Am. Mineral. 73, 741–753.
Arai, S., Miura, M., 2015. Podiform chromitites do form beneath mid-ocean ridges. Lithos 232, 143–149.
Arai, S., Yurimoto, H., 1995. Possible sub-arc origin of podiform chromitites. Isl. Arc 4, 104–111.
Arai, S., Kadoshima, K., Morishita, T., 2006. Widespread arc-related melting in the mantle section of the northern Oman ophiolite as inferred from detrital chromian magnesiochromites. J. Geol. Soc. 163, 869–879.
Arai, S., 1992. Chemistry of chromian spinel in volcanic rocks as a potential guide to magma chemistry. Mineral. Mag. 56, 173–784.
Arai, S., 1994. Compositional variation of olivine-chromian spinel in Mg-rich magma as a guide to their residual spinel peridotites. J. Volcanol. Geotherm. Res. 59, 279–294.
Arai, S., 2011. Chemical characteristics of chromian spinel in plutonic rocks: implications for deep magma processes and discrimination of tectonic setting. Isl. Arc 20, 125–137.
Aswad, K.J., Aziz, N.R., Koyi, H.A., 2011. Cr-spinel compositions in serpentinites and their implications for the petrotectonic history of the Zagros Suture Zone Kurdistan Region. Iraq Geol. Mag. 148, 802–818.
Barnes, S.J., Roeder, P.L., 2001. The range of spinel compositions in terrestrial mafic and ultramafic rocks. J. Petrol. 42, 2279–2302.
Barnes, S.J., 2000. Chromite in komatiites, II: Modification during greenschist to mid-amphibolite facies metamorphism. J. Petrol. 41, 387–409.
Bhat, I.M., Ahmad, T., Subba Rao, D.V., 2017. Geochemical characterization of serpentinized peridotites from the Shergol ophiolitic slice along the Indus Suture Zone (ISZ), Ladakh Himalaya, India. J. Geol. 125, 501–513.
Bodinier, J.L., Godard, M., 2003. Orogenic, ophiolitic and abyssal peridotites. In: In: Carlson, R.W. (Ed.), Treatise on Geochemistry Vol. 2. Elsevier, Amsterdam, pp. 103–170.
Bonatti, E., Michael, P.J., 1989. Mantle peridotites from continental rifts to oceanic basins to subduction zones. Earth Planet Sci. Lett. 91, 297–311.
Brookfield, M.E., Reynolds, P.H., 1981. Late Cretaceous emplacement of the Indus suture zone ophiolitic melanges and an Eocene-Oligocene magmatic arc on the northern edge of the Indian plate. Earth Planet. Sci. Lett. 55, 157–162.
Cabanes, N., Mercier, J.C.C., 1988. Insight into the upper mantle beneath an active extensional zone: the spinel-peridotite xenoliths from San Quentin (Baja California, Mexico). Contrib. Mineral. Petrol. 100, 374–382.
Cannat, M., Mascle, G., 1990. Réunion extraordinaire de la société géologique de France en Himalaya du Ladakh. Bull. Soc. Geol. Fr. 4, 553–582.
Choi, S.H., Shervais, J.W., Mukasa, S.B., 2008. Supra-subduction and abyssal mantle peridotites of the Coast Range ophiolite. California.Contrib. Mineral. Petrol. 156, 551–576.
Cimen, O., Koksal, F.T., Onal, A.O., Aktag, A., 2016. Depleted to refertilized mantle peridotites hosting chromites within the Tunceli ophiolite, Eastern Anatolia (Turkey): Insights on the back arc origin. Ofioliti 41, 1–20.
Clift, P.D., Degnan, P.J., Hannigan, R., Blusztajn, J., 2000. Sedimentary and geochemical evolution of the Dras fore arc basin Indus suture, Ladakh Himalaya. India Geol. Soc. Am. Bull. 112, 450–466.
Corfield, R.I., Searle, M., Green, O., 1999. Photang thrust sheet, an accretionary complex structurally below the Spontang ophiolite constraining timing and tectonic environment of ophiolite obduction, Ladakh Himalaya, NW India. J. Geol. Soc. Lond. 156, 1031–1044.
Corfield, R.I., Searle, M.P., Pedersen, R.B., 2001. Tectonic setting and obduction history of the Spontang ophiolite, Ladakh Himalaya, NW India. J. Geol. 109, 715–736.
Dare, S.A.S., Pearce, J.A., McDonald, I., Styles, M.T., 2009. Tectonic discrimination of peridotites using fO_2-Cr-number and Ga-Ti-Fe^{III} systematics in chrome-spinel. Chem. Geol. 261, 199–216.
Deer, W.A., Howei, R.A., Zussman, J., 1992. The Rock Forming Minerals, second ed. Longmans, London (696pp).
Delavari, M., Amini, S., Saccani, E., Beccaluva, L., 2009. Geochemistry and petrogenesis of mantle peridotites from the Nehbandan Ophiolitic Complex, eastern Iran. J. Appl. Sci. 9, 2671–2687.
Dick, H.J.N., Bullen, T., 1984. Chromian spinel as a petrogenetic indicator in abyssal and alpine-type peridotites and spatially associated lavas. Contrib. Mineral. Petrol. 86,

54–76.
Edwards, S.J., Malpas, J., 1995. Multiple origins for mantle harzburgites: examples from the Lewis Hills, Bay of Islands Ophiolite, Newfoundland. Can. J. Earth Sci. 32, 1046–1057.
Farahat, E.S., 2008. Chrome-spinels in serpentinites and talc carbonates of the El Ideid-El Sodmein District, central Eastern Desert, Egypt: their metamorphism and petrogenetic implications. Chem. Erde Geochem. 68, 193–205.
Frank, W., Gansser, A., Trommsdorff, V., 1977. Geological observations in the Ladakh area (Himalayas)-a preliminary report. Schweiz. Mineral. Petrogr. Mitt. 57, 89–113.
Gansser, A., 1964. The Geology of the Himalayas. Wiley-Interscience, New York (289pp).
Gansser, A., 1980. The significance of the Himalaya suture zone. Tectonophysics 62, 37–40.
Hattori, K.H., Guillot, S., 2007. Geochemical character of serpentinites associated with high to ultrahigh pressure metamorphic rocks in the Alps, Cuba and the Himalayas: recycling of elements in subduction zones. Geochem. Geophys. Geosyst. 8, 1–27.
Hellebrand, E., Snow, J.E., Dick, H.J., Hofmann, A.W., 2001. Coupled major and trace elements as indicators of the extent of melting in mid-ocean-ridge peridotites. Nature 410, 677–681.
Hellebrand, E., Snow, J.E., Hoppe, P., Hofmann, A.W., 2002. Garnet field melting and late stage refertilization in residual abyssal peridotites from the Central Indian ridge. J. Petrol. 43, 2305–2338.
Honegger, K., Dietrich, V., Frank, W., Gansser, A., Thoni, M., Trommsdorf, V., 1982. Magmatic and metamorphism in the Ladakh Himalayas (the Indus-Tsangpo suture zone). Earth Planet. Sci. Lett. 60, 253–292.
Honegger, K., Le Fort, P., Mascle, G., Zimmermann, J.L., 1989. The blueschists along the indus suture zone in ladakh, NW himalaya. J. Metamorph. Geol. 7, 57–72.
Irvine, T.N., 1967. Cr-spinel as a petrogenetic indicator, part 2 − petrological applications. Can. J. Earth Sci. 4, 71–103.
Ishii, T., Robinson, P.T., Maekawa, H., Fiske, R., 1992. Petrological studies of peridotites from diapiric serpentinite seamounts in the Izu-Ogasawara-Mariana fore arc, Leg 125. In: Proceedings of the Ocean Drilling Program, Scientific Results. College Station, Texas, USA. pp. 445–485.
Jan, M.Q., Windley, B.F., 1990. Chromian spinel silicate chemistry in ultramafic rocks of the Jijal complex, northwestern Pakistan. J. Petrol. 31, 667–715.
Kamenetsky, V.S., Crawford, A.J., Meffre, S., 2001. Factors controlling chemistry of magmatic spinel: an empirical study of associated olivine, Cr-spinel and melt inclusions from primitive rocks. J. Petrol. 42, 655–671.
Kapsiotis, A.I., Tsikouras, B.T., Grammatikopoulos, T., Karipi, S.T., Hatzipanagiotou, K., 2007. On the metamorphic modification of Cr-spinel compositions from the ultrabasic rocks of the Pindos ophiolite complex (NW Greece). Bull. Geol. Soc. Greece 40, 781–793.
Karipi, S., Tsikouras, B., Hatzipanagiotou, K., 2007. Petrogenetic significance of spinel-group minerals from the ultramafic rocks of the Iti and Kallidromon ophiolite (Central Greece). Lithos 99, 136–149.
Kelemen, P.B., Shimizu, N., Salters, V.J.M., 1995. Extraction of MORB from the upwelling mantle by focused flow of melt in dunite channels. Nature 375, 747–753.
Kimball, K.L., 1990. Effects of hydrothermal alteration on the compositions of chromian spinels. Contrib. Mineral. Petrol. 105, 337–346.
Lee, Y.I., 1999. Geotectonic significance of detrital chromian spinel: a review. Geosci. J. 3, 23–29.
Mahéo, G., Bertrand, H., Guillot, S., Villa, I.M., Keller, F., Capiez, P., 2004. The south Ladakh ophiolites (NW Himalaya, India): an intra-oceanic tholeiitic origin with implication for the closure of the Neo-Tethys. Chem. Geol. 203, 273–303.
Maheo, G., Fayoux, X., Guillot, S., Garzanti, E., Capiez, P., Mascle, G., 2006. Relicts of an intra-oceanic arc in the Sapi-Shergol mélange zone (Ladakh, NW, Himalaya, India): implications for the closure of the Neo-Tethys Ocean. J. Asian Earth Sci. 26, 695–707.
Matsumoto, I., Arai, S., Yamauchi, H., 1997. High-Al podiform chromitites in dunite-harzburgite complexes of the Sangun zone Central Chugoku district, Southwest Japan. J. Asian Earth Sci. 15, 295–302.
Melcher, F., Grum, W., Simon, G., Thathammer, V.T., Stumpfl, E.F., 1997. Petrogenesis of the ophiolitic giant chromite deposits of Kempirsai, Kazakhstan-a case study of solid and fluid inclusion in chromites. J. Petrol. 38, 1419–1458.
Ningthoujam, P.S., Dubey, C.S., Guillot, S., Fagion, A.S., Shukla, D.P., 2012. Origin and serpentinization of ultramafic rocks of Manipur Ophiolitic Complex in the Indo Myanmar subduction zone, Northeast India. J. Asian Earth Sci. 50, 128–140.
Niu, Y., Langmuir, C.H., Kinzler, R.J., 1997. The origin of abyssal peridotites: a new perspective. Earth Planet. Sci. Lett. 152, 251–265.
Niu, Y., 1997. Mantle melting and melt extraction processes beneath ocean ridges: evidence from abyssal peridotites. J. Petrol. 38, 1047–1074.
Niu, Y., 2004. Bulk-rock major and trace element compositions of abyssal peridotites: implications for mantle melting, melt extraction and post-melting processes beneath mid-ocean ridges. J. Petrol. 45, 2423–2458.
Paraskevopoulos, G.M., Economou, M., 1980. Genesis of magnetite ore occurrences by metasomatism of chromite ores in Greece. Neues Jahrb. Mineral. Abh. 140, 29–53.
Parkinson, I.J., Pearce, J.A., 1998. Peridotites from the Izu-Bonin-Mariana forearc (ODP Leg 125): evidence for mantle melting and melt-mantle interaction in a supra-subduction zone setting. J. Petrol. 39, 1577–1618.
Pearce, J.A., Barker, P.F., Edwards, S.J., Parkinson, I.J., Leat, P.T., 2000. Geochemistry and tectonic significance of peridotites from the South Sandwich arc-basin system, south Atlantic. Contrib. Mineral. Petrol. 139, 36–53.
Pedersen, R.B., Searle, M.P., Corfield, R.I., 2001. U–Pb zircon ages from the spontang ophiolite, ladakh himalaya. J. Geol. Soc. Lond. 158, 513–520.
Raz, U., Honegger, K., 1989. Magmatic and tectonic evolution of the Ladakh Block from field studies. Tectonophysics 161, 107–118.
Reuber, I., Montigny, R., Thuizat, R., Heitz, A., 1990. K/Ar ages of ophiolites and arc volcanics of the Indus Suture Zone: comparison with other Himalaya-Karakorum data. Himalayan Geol. 1, 115–125.
Reuber, I., 1986. Geometry of accretion and oceanic thrusting of Spontang ophiolite, Ladakh-Himalaya. Nature 321, 592–596.
Rizeli, M.R., Beyarslan, M., Wang, K.L., Bingol, A.F., 2016. Mineral chemistry and petrology of mantle peridotites from the Guleman ophiolite (SE Anatolia, Turkey): Evidence of a fore arc setting. J. Afr. Earth. Sci. 123, 392–402.
Robertson, A., 2000. Formation of mélanges in the Indus Suture Zone, Ladakh Himalaya by successive subduction-related, collisional, post-collisional processes during Late Mesozoic –Late Tertiary time. In: In: Khan, M.A., Treolar, P.J., Searle, M.P., Jan, Q. (Eds.), Tectonics of the Nanga Parbat Syntaxes and the Western Himalaya. Geol. Soc. Spec. Pub. 170. Geological Society of London, pp. 333–374.
Roeder, P.L., Reynold, I., 1991. Re-equilibration of Cr-spinel within the Kilauea Iki lava lake. Hawaii. Contrib. Mineral. Petrol. 107, 8–12.
Sack, R.O., Ghiorso, M.S., 1991. Chromian spinels as petrogenetic indicators: thermodynamic and petrological applications. Am. Mineral. 76, 827–847.
Scowen, P.A.H., Roeder, P.L., Helz, R.T., 1991. Re-equilibration of chromite within Kilauea Iki lava lake. Hawaii. Contrib. Mineral. Petrol. 107, 8–20.
Searle, M.P., Windley, B.F., Coward, M.P., Cooper, D.J.W., Rex, D., Tingdong, L., Xuchang, X., Jan, V.C., Thakur, V.C., Kumar, S., 1987. The closing of Tethys and the tectonics of the Himalaya. Geol. Soc. Am. Bull. 98, 678–701.
Searle, M.P., 1983. Stratigraphy, structure and evolution of the Tibetan-Tethys zone in Zanskar and the Indus suture zone in the Ladakh Himalaya: royal Society of Edinburgh Transactions. Earth Sci. 73, 205–219.
Shah, S.K., Sharma, M.L., 1977. A preliminary report on the fauna in radiolarites of the ophiolitic melange zone around Mulbekh, Ladakh. Curr. Sci. 46, 817.
Shervais, J.W., Choi, S.H., Sharp, W.D., Ross, J., Schuman, M.Z., Mukasa, S.B., 2011. Serpentinite matrix mélange: implications of mixed provenance for mélange formation. In: In: Wakabayashi, J., Dilek, Y. (Eds.), Melanges: Processes for Formation and Societal Significance 480. Geological Society of America, pp. 1–30 (Special Paper).
Shiga, Y., 1987. Behavior of iron, nickel, cobalt and sulfur during serpentinization with reference to Hayachine ultramafic rocks of the Kamaishi mining district, northeastern Japan. Can. Mineral. 25, 611–624.
Singh, A.K., 2009. High Al-chromian spinel in peridotites of Manipur Ophiolite Complex, Indo-Myanmar Orogenic Belt: implication for petrogenesis and geotectonic setting. Curr. Sci. 96, 973–978.
Sinha, A.K., Mishra, M., 1992. Emplacement of the ophiolitic mélange along continental collision zone of Indus Suture Zone in Ladakh Himalaya. J. Himalayan Geol. 3, 179–189.
Sinha, A.K., Mishra, M., 1994. The existence of oceanic islands in the Neotethys: evidence from Ladakh Himalaya. India Curr. Sci. 67, 721–727.
Thakur, V.C., 1981. Regional framework and geodynamic evolution of the Indus Tsangpo suture zone in the Ladakh Himalayas: royal Society of Edinburgh Transactions. Earth Sci. 72, 890–897.
Thalhammer, O.A.R., Prochaska, W., Muhlhans, H.W., 1990. Solid inclusions in chromespinels and platinum group element concentrations from the Hochgrossen and Kraubath ultramafic massifs (Austria): Their relationships to metamorphism and serpentinization. Contrib. Mineral. Petrol. 105, 66–80.
Virdi, N.S., Thakur, V.C., Kumar, S., 1977. Blueschist facies metamorphism from the Indus suture zone of Ladakh and its significance. Himalayan Geol. 7, 479–482.
Wylie, A.G., Candela, P.A., Burke, T.M., 1987. Compositional zoning in unusual Zn-rich chromite from the Sykeville district of Maryland and its bearing on the origin of the ferritchromite. Am. Mineral. 72, 413–422.
Xiong, F., Yang, J., Ba, D.Z., Liu, Z., Xu, X.Z., Feng, G., Niu, X., Xu, J., 2014. Different type of chromitite and genetic model from Luobusa ophiolite. Tibet. Acta Petrol. Sin. 30, 2137–2163.
Xiong, F., Yang, J., Robinson, P.T., Xu, X.Z., Liu, Z., Li, Y., Li, J., Chen, Y., 2015. Origin of podiform chromitite, a new model based on the Luobusa ophiolite, Tibet. Gondwana Res. 27, 525–542.
Xiong, F., Yang, J., Robinson, P.T., Gao, J., Chen, Y., Lai, S., 2017a. Petrology and geochemistry of peridotites and podiform chromitite in the Xigaze ophiolite, Tibet: implications for a suprasubduction zone origin. J. Asian Earth Sci. 146, 56–75.
Xiong, F., Yang, J., Robinson, P.T., Xu, X.Z., Zhou, W., Feng, G., Xu, J., Li, J., Niu, X., 2017b. High-Al and high-Cr podiform chromitites from the western Yarlung-Zangbo suture zone, Tibet: implications from mineralogy and geochemistry of chromian spinel, and platinum-group elements. Ore Geol. Rev. 80, 1020–1041.
Zhou, M.F., Kerrich, R., 1992. Morphology and composition of Cr-spinel in komatiites from the Belingwe greenstone belt. Zimbabwe. Can. Mineral. 30, 303–317.
Zhou, M.F., Robinson, P.T., Bai, W.J., 1994. Formation of podiform chromitites by melt/rock interaction in the upper mantle. Mineral. Deposita 29, 98–101.
Zhou, M.F., Robinson, P.T., Malpas, J., Li, Z., 1996. Podiform chromitites in the Luobusa ophiolite (southern Tibet): implications for melt-rock interaction and chromite segregation in the upper mantle. J. Petrol. 37, 3–21.
Zhou, M.F., Lightfoot, P.C., Keays, R.R., Moore, M.L., Morrison, G.G., 1997. Petrogenetic significance of chromian spinels from the subury igneous complex Ontario. Can. Can. J. Earth Sci. 34, 1405–1419.
Zhou, M.F., Robinson, P.T., Malpas, J., Edwards, S.J., Qi, L., 2005. REE and PGE geochemical constraints on the formation of dunites in the Luobusa ophiolite, southern Tibet. J. Petrol. 46, 615–639.
Zhou, M.F., Robinson, P.T., Su, B.X., Gao, J.F., Li, J.W., Yang, J.S., Malpas, J., 2014. Compositions of chromite, associated minerals, and parental magmas of podiform chromite deposits: the role of slab contamination of asthenospheric melts in suprasubduction zone environments. Gondwana Res. 26, 262–283.
de Sigoyer, J., Chavagnac, V., Blichert-Toft, J., Villa, I.M., Luais, B., Guillot, S., Cosca, M., Mascle, G., 2000. Dating the Indian continental subduction and collisional thickening in the northwest Himalaya: multichronology of the Tso Morari eclogites. Geology 28, 487–490.